· Article · Advances in Polar Science
doi:10.12429/j.advps.2025.0011 December 2025 Vol. 36 No. 4: 345-355

Changes in bacterial community structure along a slope in sparse tundra soil near the Antarctic coast

WANG Jun[1], LIU Long[2], ZHAO Yunxia[2], ZHANG Xinyuan[2], XU Xiaoyu[2], ZHU Xiaofeng[2], KONG Lingkai[2], CAO Huansheng[3], WANG Nengfei[2] & DU Jiawen[2*]

[1] School of Life Sciences, Linyi University, Linyi 276000, China;
[2] School of Chemistry and Chemical Engineering, Linyi University, Linyi 276000, China;
[3] Division of Natural and Applied Sciences, Duke Kunshan University, Suzhou 215316, China

Received 17 May 2025; accepted 18 August 2025; published online 30 December 2025

Abstract Research on Antarctic microbial diversity has primarily focused on 3 areas: freshwater lake sediments, penguin colonies, and seawater in ice-free regions. There is a scarcity of research on the impact of slopes on microbial community structure, and this study effectively fills this gap. This study focused on the soil in the sparse vegetated tundra on a hillside near the southern coastline of the Antarctic Great Wall Station. The influence of slope position, soil physicochemical properties, and vegetated area on soil bacterial community structure was analyzed. High-throughput sequencing technology was employed to characterize a 16S rRNA gene fragment in soil samples from 5 slope areas and estimate bacterial abundance. Calculation of α-diversity and β-diversity indices, and community structure analysis were used to compare the species richness among sampling points, analyze similarities in soil bacterial community structure and composition, and identify the core bacterial population. In the non-vegetated area, the soil on the mountaintop, hillside, and at the foot of the slope showed similar physicochemical properties. In the vegetated area, the soil physicochemical properties were highly similar on the mountaintop, hillside, the foot of the slope, and the foot of the mountain. Weighted Gene Co-expression Network Analysis showed that total organic carbon, pH, and PO_4^{3-}-P might affect the structure of bacterial communities at the sampling point by changing the relative abundance of Chthoniobacterales, *Sediminibacterium*, and *Actinobacteria*. We hypothesize that slope-driven nutrient transport, amplified by vegetated areas (in the tundra), is a primary driver of bacterial community structure in the Antarctic tundra soil. These results provide insights into the impact of slope on microbial community structure in Antarctica.

Keywords **Antarctic, high-throughput sequencing, WGCNA, bacterial diversity, soil physicochemical properties**

Citation: Wang J, Liu L, Zhao Y X, et al. Changes in bacterial community structure along a slope in sparse tundra soil near the Antarctic coast. Adv Polar Sci, 2025, 36(4): 345-355, doi:10.12429/j.advps.2025.0011

1 Introduction

Antarctica plays a pivotal role in regulating the global climate (Colesie et al., 2023). The Fildes Peninsula is the largest ice-free area in Antarctica and hosts 6 permanent bases (Henriques et al., 2018), including China's Antarctic Great Wall Station. To date, research on Antarctic microbial diversity has mainly focused on sediments of freshwater lakes (Roldán et al., 2022), penguin colonies (Wang et al., 2015), and seawater in ice-free areas (Zhang et al., 2022). Relatively few studies have investigated the microbial communities on slopes in ice-free areas. Therefore, investigating the microbial community structure on the ice-free slopes of the Fildes Peninsula is crucial to gain a

* Corresponding author. E-mail: dujiawen0919@163.com

broad understanding of the microbial diversity of Antarctica.

The nearshore area of the Fildes Peninsula has limited flat terrain and an undulating topography, which is a typical landform in the Antarctic nearshore zone. This landscape is covered with vegetated tundra. The coastal areas of Antarctica are predicted to experience extended rainfall events and shorter rainfall intervals by the end of this century (Vignon et al., 2021). Frequent and prolonged rainfall will have far-reaching impacts on the ecological environment of Antarctica. The coastal areas are critical habitats for Antarctic vegetation. The vegetation comprises mainly lichens, while mosses and algae also constitute a substantial proportion (Singh et al., 2018). Mosses and lichens, as the dominant vegetation in alpine and polar ecosystems, are highly resilient to harsh environments (Asplund et al., 2022), and play an important role in stabilizing the nutrient cycling and energy flow within terrestrial ecosystems (Qu et al., 2024). Given that soil available moisture content (MC) will affect the survival and growth of lichens and mosses (Perera-Castro et al., 2020), the increase in MC resulting from the more frequent rainfall may further increase vegetation coverage in the coastal areas of Antarctica. Vegetation coverage has a significant impact on certain soil physicochemical properties (Maria Teixeira Lins et al., 2023), while soil physicochemical properties such as pH (Lebre et al., 2023), nitrate nitrogen (Wang et al., 2021), salinity (Dong et al., 2023), available phosphorus (Samaddar et al., 2019), carbon (Li et al., 2025), and temperature (Ji et al., 2024) can affect the bacterial community structure in the soil. The soil in Antarctica is mostly loose in texture and structure. Frequent rainfall can facilitate the transport of dissolved nutrients and some microorganisms may be transported with soil particles. Therefore, the frequent rainfall in Antarctica anticipated in the future will directly or indirectly affect the local microbial community structure. On the sloped terrain, frequent rainfall enhanced nutrient transport will be obvious. Consequently, research on the link between slope position, nutrient transport and bacterial communities offers insights into Antarctic nearshore ecosystem responses to more rainfall.

This study aims to explicitly address the following core objectives: (1) evaluate differences in the bacterial community structure between the upper- and lower-slope areas, as well as the causes of such differences; (2) assess differences in the bacterial community structure between vegetated and non-vegetated areas and their causes; and (3) identify the core bacterial community at the sampling points and the soil physicochemical properties that determine the bacterial community structure at the sampling points.

2 Materials and methods

2.1 Sampling locations and sample collection

The samples were collected from a hillside near the southern coastline of China's Great Wall Station in Antarctica. The sampling site is located on the Fildes Peninsula in the southwest of King George Island. As a pristine continent, Antarctica serves as an ideal location for investigating the spatial transport of environmental pollutants and anthropogenic environmental impacts (Gao et al., 2018). In February 2018, following a rain event, soil samples were collected from 9 locations (Figure 1 and Table 1). Four sampling points were situated in a non-vegetated area: WZB1 (mountaintop), WZB2 (hillside), WZB3 (foot of the slope), and WZB4 (foot of the mountain). An additional site in the non-vegetated area, WZB5, was selected where rainwater from a vegetated area accumulated. Four sites were located in the vegetated area: ZB1 (mountaintop), ZB2 (hillside), ZB3 (foot of the slope), and ZB4 (foot of the mountain). In addition to the soil samples collected from the 9 sites, biological samples of lichens and mosses were also collected from the vegetated areas, including the surface rinse samples of lichen (designated as DYC), the nitrogen-ground samples of lichens (designated as DYF), the surface rinse samples of moss (designated as TXC), and the liquid nitrogen-ground samples of mosses (designated as TXF).

Table 1 Details for the sample collection sites

Sites	Location Profile	Latitude	Longtitude
WZB1	soil on the mountaintop in the non-vegetated area	62.2217°S	58.9472°W
WZB2	soil on the hillside in the non-vegetated area	62.2217°S	58.9469°W
WZB3	soil at the foot of the slope in the non-vegetated area	62.2217°S	58.9467°W
WZB4	soil at the foot of the mountain in the non-vegetated area	62.2217°S	58.9464°W
WZB5	soil after the rainwater flows from the vegetation-covered area to the non-vegetated area	62.2214°S	58.9464°W
ZB1	soil on the mountain top in the vegetated area	62.2222°S	58.9472°W
ZB2	soil on the hillside in the vegetated area	62.2222°S	58.9469°W
ZB3	soil at the foot of the slope in the vegetated area	62.2222°S	58.9467°W
ZB4	soil at the foot of the mountain in the vegetated area	62.2222°S	58.9464°W

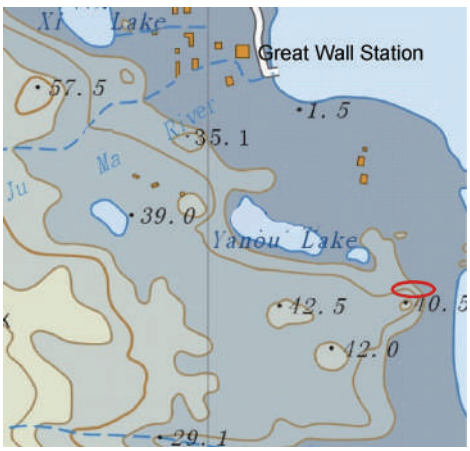

Figure 1 Map of the sampling site locations. The specific sampling area is marked with red circle.

Using pre-sterilized spoons, 3 parallel topsoil samples from approximately 5 cm depth below the soil surface were collected at each site, and placed into sterile bags. All collected samples were immediately stored at −20 ℃ and then transferred to an ultra-low-temperature freezer (−80 ℃) for storage.

2.2 Soil physicochemical properties

A total of 8 soil physicochemical properties were measured, comprising MC, pH, total organic carbon (TOC), NH_4^+-N, SiO_3^{2-}-Si, PO_4^{3-}-P, NO_3^--N and NO_2^--N. The MC of the soil samples was determined by the drying method. Briefly, the samples were placed in a drying oven at 105 ℃ and dried to constant weight. The mass of the samples was then weighed and the water loss was calculated (Li et al., 2022). For pH measurement, 10 mL distilled water was added to 4 g soil, and the pH was then measured with a pH electrode (PHS-3C, Shanghai REX Instrument Factory, Shanghai, China). The TOC content was determined with a Vario MAX CN analyzer (Elementar, Langenselbold, Germany) (Kobierski et al., 2020). The NH_4^+-N, SiO_3^{2-}-Si, PO_4^{3-}-P, NO_3^--N and NO_2^--N concentrations were measured using a High Performance Microflow Analyzer (QuAAtro, SEAL Analytical GmbH, Norderstedt, Germany).

2.3 DNA extraction and PCR amplification

DNA was extracted from soil samples, rinse samples of mosses and lichens, and liquid nitrogen-ground samples of mosses and lichens using the Mo Bio PowerSoil DNA Isolation Kit (MO BIO Laboratories, San Diego, CA, USA). The operating procedure was strictly followed according to the manufacturer's instructions. Amplification of the V3–V4 region of the 16S rRNA gene was performed using the universal bacterial primers 341F (5'-CCTAYGGGRB GCASCAG-3') and 806R (5'-GGACTACNNGGGTAT CTAAT-3') (Niem et al., 2020). The PCR conditions were as follows: initial denaturation at 98 ℃ for 1 min; followed by 30 cycles of denaturation at 98 ℃ for 10 s, annealing at 50 ℃ for 10 s, and extension at 72 ℃ for 60 s; and final extension at 72 ℃ for 5 min (Zhao et al., 2017). PCR products with an amplification signal between 400 and 450 bp were selected for purification using the GeneJET Gel Extraction Kit, and then used for high-throughput sequencing.

2.4 High-throughput sequencing and data analysis

High-throughput sequencing was performed on the purified PCR product libraries (the V3–V4 region of the 16S rRNA gene) on the Illumina MiSeq platform (Qin et al., 2023). The raw sequences comprised 250 bp paired-end reads.

To clean the raw reads, we used QIIME (version 1.8.0) to filter out low-quality bases, followed by comparison with Silva database to identify and eliminate chimeric sequences. Using UPARSE (version 7.0), the clean reads from all samples were clustered into operational taxonomic units (OTUs) at a 97% sequence similarity threshold. The most abundant sequence within each OTU was defined as the representative sequence. Species annotation and analysis were conducted on the OTU representative sequences with QIIME in conjunction with the SILVA rRNA database (version 138) (Xiang et al., 2020). The analytical methods used include α-diversity analysis, β-diversity analysis, community composition and structure analysis, and principal component analysis (PCA). The clean reads were submitted to the NCBI Sequence Read Archive database (accession numbers: SAMN48407964–SAMN48408002).

QIIME (version 2.0) was used to calculate four α-diversity (ACE, Chao1, Shannon, and Simpson) and β-diversity indices and conduct community structure analysis. Weighted Gene Co-expression Network Analysis (WGCNA) was conducted using RStudio (version 4.0.5) to analyze the correlations between the soil physicochemical properties and the bacterial community structure and to identify the core bacterial community.

3 Results

3.1 Comparison of soil physicochemical properties among sampling points

The soil physicochemical properties at the sampling points in the non-vegetated area (WZB1, WZB2, WZB3, WZB4, and WZB5) and the vegetated area (ZB1, ZB2, ZB3, and ZB4) were analyzed. In the non-vegetated area, the MC gradually increased with the decrease in the slope, but the opposite trend was observed in the vegetated area (Figure 2). A similar pattern was observed for TOC, which gradually increased in the non-vegetated area, but decreased in the vegetated area, with decrease in the slope. The content of SiO_3^{2-}-Si in the soil was significantly higher at WZB5, which received rainwater runoff from the vegetated area, than that at all other sampling points. The content of NO_3^--N in the soil on the mountaintop of the vegetated area (ZB1) was the highest among all sampling points. The soil pH on the mountaintop and hillside in the non-vegetated area was significantly higher than at the other sampling points. The content of NH_4^+-N in the hillside soil of the non-vegetated area was significantly the highest among the sampling points. The content of PO_4^{3-}-P in soil on the hillside of the vegetated area was significantly higher than at the other sampling points. The content of NO_2^--N in the mountaintop soil of the non-vegetated area was the highest among the sampling points. Furthermore, significant differences were observed when all sampling points were grouped into the vegetated and non-vegetated areas. The

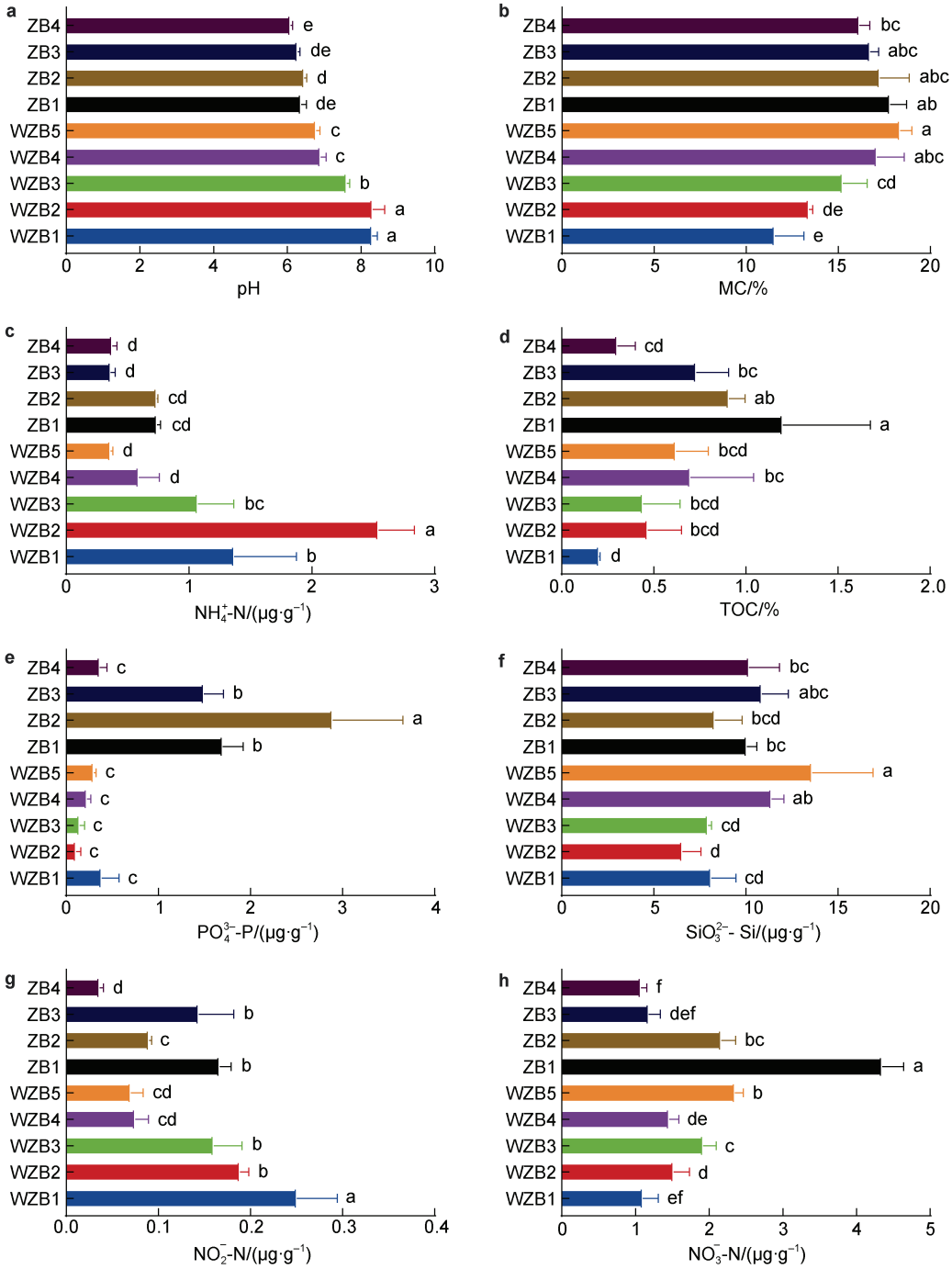

Figure 2 Analysis of soil physicochemical properties at the 9 sampling points. Different lowercase letters beside the bars indicate significant differences at 0.05 level. **a**, pH; **b**, MC; **c**, NH_4^+-N; **d**, TOC; **e**, PO_4^{3-}-P ; **f**, SiO_3^{2-}-Si ; **g**, NO_2^--N; **h**, NO_3^--N .

vegetated area had significantly higher contents of TOC, NO_3^--N , and PO_4^{3-}-P , whereas the non-vegetated area had significantly higher contents of NH_4^+-N and NO_2^--N .

PCA was performed on the soil physicochemical properties data to evaluate similarities among the sampling points. The first and second principal components collectively accounted for 92.75% of the total variance (Figure 3), indicating that the total variation in the dataset was adequately represented in two dimensions. Relatively strong similarities in the physicochemical properties at WZB1, WZB2, and WZB3 in the non-vegetated area were indicated, while relatively high similarities in the physicochemical properties at ZB1, ZB2, ZB3, and ZB4 in the vegetated area were observed.

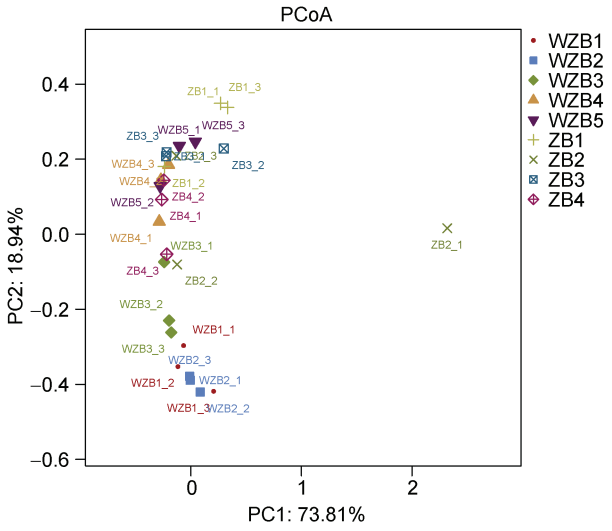

Figure 3 Principal component analysis scatterplot of soil physicochemical properties at each sampling point.

3.2 Analysis of bacterial community diversity and structure

The 9 soil samples and 4 biological samples of lichens and mosses have been analyzed. A total of 7,018 OTUs were resolved and four α-diversity and β-diversity indices were calculated. The ACE and Chao1 indices were calculated to describe the species richness, while the Shannon and Simpson indices were used to describe the evenness or relative diversity of species. The WZB5 samples had the highest ACE and Chao1 index values among all sampling points (Table 2), indicating that the site had the highest species richness. Moreover, WZB5 had the highest Shannon index and lowest Simpson index values, suggesting that the site also had the highest species diversity. The coverage values for all samples ranged from 0.987 to 0.995, indicating that the sequencing depth was sufficient to detect a majority of the bacterial populations in the samples.

Table 2 The α-diversity indices for the bacterial community detected at each sampling point

Sampling site	Ace	Chao1	Shannon	Simpson	Coverage
WZB1	2297.430±141.933	2328.520±160.733	5.999±0.189	0.005±0.001	0.990±0.001
WZB2	2549.253±253.644	2575.518±260.528	5.961±0.271	0.009±0.005	0.991±0.003
WZB3	2693.668±97.081	2710.899±106.431	6.214±0.044	0.005±0.001	0.987±0.001
WZB4	3085.896±167.376	3103.696±165.162	6.400±0.191	0.004±0.001	0.987±0.001
WZB5	3596.116±126.141	3636.982±128.898	6.598±0.040	0.004±0.000	0.987±0.003
ZB1	3401.537±109.401	3439.994±130.908	5.990±0.183	0.010±0.005	0.988±0.002
ZB2	2884.242±586.525	2946.667±615.434	5.385±1.270	0.048±0.056	0.987±0.005
ZB3	3041.041±189.056	3087.824±184.001	6.207±0.174	0.007±0.003	0.988±0.003
ZB4	3170.865±190.052	3208.709±220.293	6.132±0.139	0.009±0.002	0.989±0.002
DYC	1794.323±394.630	1885.456±411.768	4.296±0.557	0.068±0.034	0.995±0.001
DYF	3007.022±83.160	3090.192±113.267	6.285±0.038	0.009±0.006	0.989±0.001
TXC	1725.149±541.368	1806.878±525.368	5.069±0.444	0.017±0.007	0.992±0.001
TXF	2647.578±293.096	2694.407±326.665	5.936±0.577	0.010±0.007	0.988±0.003

After excluding the unclassified bacteria, sequences from all sites were broadly categorized into 14 dominant phyla (Figure 4a). Excluding the sites in the non-vegetated area, the relative abundance of Proteobacteria at the vegetated sampling sites was significantly higher than that of other phyla. In the non-vegetated area, Proteobacteria and Acidobacteria were dominant, whereas in the vegetated area, Proteobacteria were dominant. With consideration of slope height, in the non-vegetated area, Proteobacteria and Acidobacteria were dominant regardless of the slope height. In the vegetated area, Proteobacteria were dominant in the upper-slope area, whereas in the lower-slope area, the proportions of Proteobacteria, Acidobacteria, Actinomycetes, and Campylobacterota were approximately comparable, and no dominant phylum was discernible in terms of relative abundance. Considering the surface-associated and internal bacteria associated with lichens and mosses, the relative abundance of Proteobacteria was significantly higher than that of other bacterial phyla. Except at ZB1 and ZB2 of the vegetated area, where Sphingomonadaceae was dominant, the relative abundance of Gemmatimonadaceae was highest at the remaining sampling points (Figure 4b).

A PCA of the similarity in bacterial community composition among the sampling points was conducted. The first and second principal components collectively explained 66.53% of the total variance, indicating the bacterial community data were reasonably represented in two dimensions (Figure 5). The correspondence among replicate samples at the same sampling point was relatively high, indicating that within-site variation was well controlled during sampling. The bacterial community structure differed markedly between the non-vegetated and

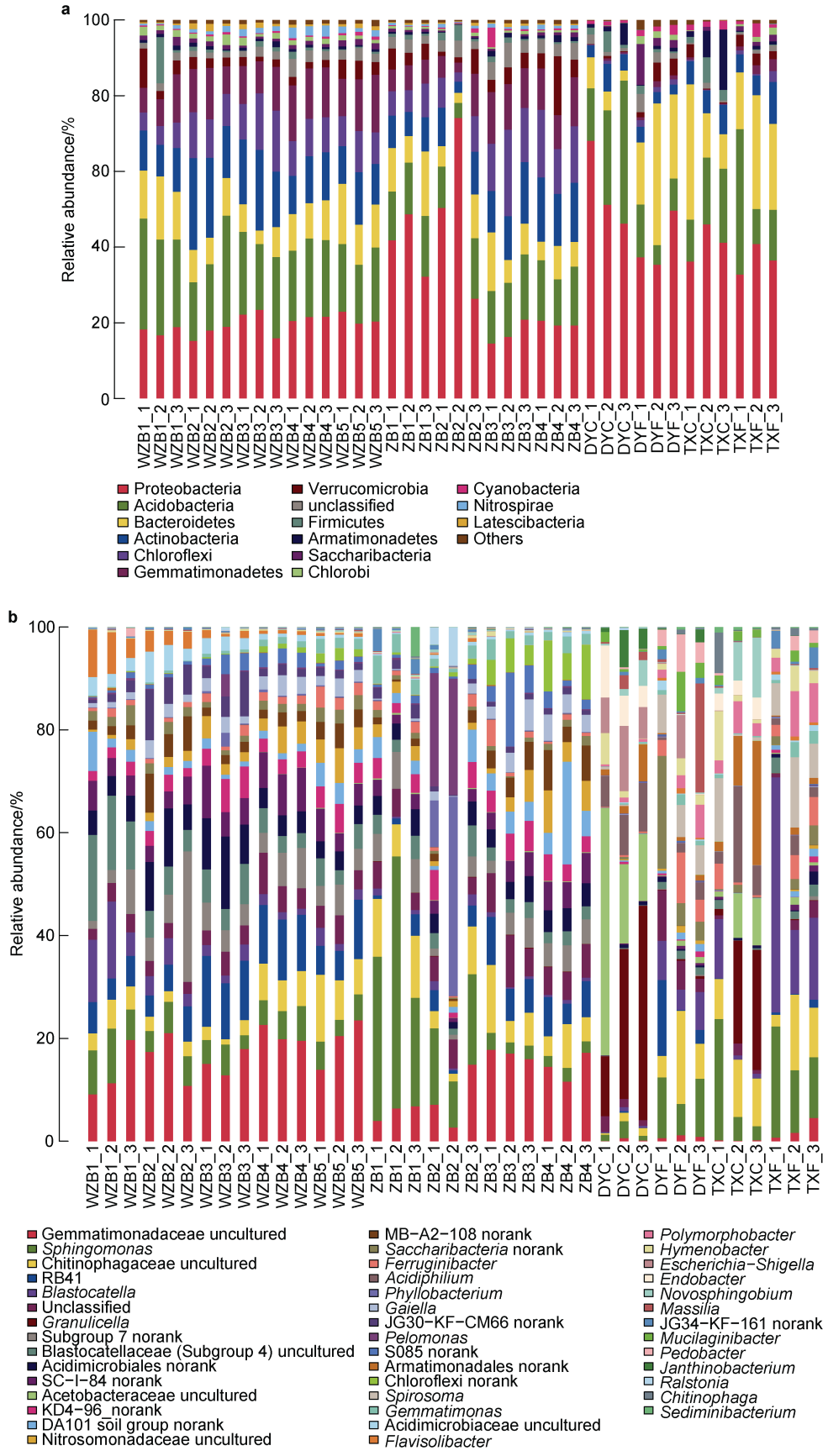

Figure 4 Bacterial community structure at the phylum level (**a**) and genus level (**b**) at each sampling point.

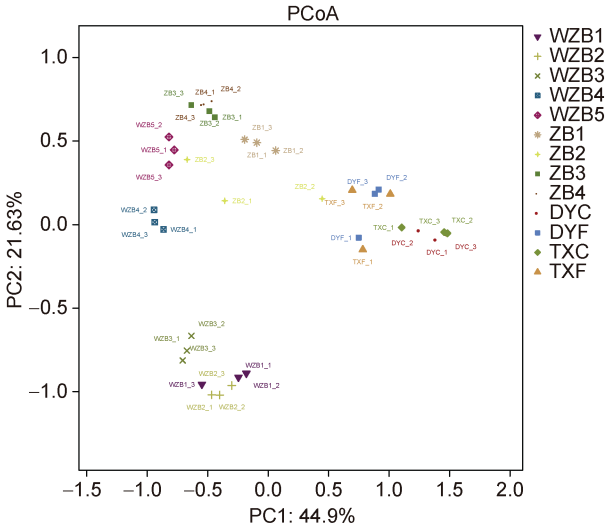

Figure 5 Principal component analysis scatterplot of bacterial community composition at each sampling point.

vegetated areas. In the non-vegetated area, differences in the community composition between the upper- and lower-slope area were indicated to a certain degree, whereas no notable differences in community composition were indicated among sampling sites in the vegetated area.

3.3 Relationship between soil physicochemical properties and bacterial community structure

The primary goal of applying the WGCNA method was to identify microbial clusters and to estimate the correlation of the clusters with environmental parameters. The microorganisms at each sampling point were clustered into 9 modules based on the similarity of their OTU abundance variation trends. Among the soil physicochemical properties, TOC (r=0.73, P<0.01) and PO_4^{3-}-P (r=0.81, P<0.01) showed a very strong correlation with the brown module, and pH (r=0.76, P <0.01) was strongly positively correlated with the turquoise module (Figure 6). Therefore, these three soil physicochemical properties might affect the bacterial community structure at the sampling points by changing the relative abundance of the key bacterial groups in the brown and turquoise modules.

The WGCNA results for each of the brown and turquoise modules were visualized as a network diagram (Figure 7). The turquoise module comprised two core bacterial taxa, namely, Chthoniobacterales and *Sediminibacterium*. The brown module included one core bacterial taxon, *Actinobacteria*.

4 Discussion

4.1 Factors influencing bacterial community structure

The soil ecosystem in Antarctica is characterized by high vulnerability, simple structure, and low resilience owing to the extreme environmental conditions, such as low temperatures, aridity, and nutrient scarcity. Climate change may result in marked changes in local biodiversity and the functions of microorganisms in the soil. Microbial communities capable of performing vital activities to produce nutrient salts are crucial for the polar ecosystem (de Scally et al., 2016). After rainfall, water flow will transport dissolved nutrients and microbial communities in the soil from upper-slope areas to lower-slope areas, thereby changing the structure of the microbial community.

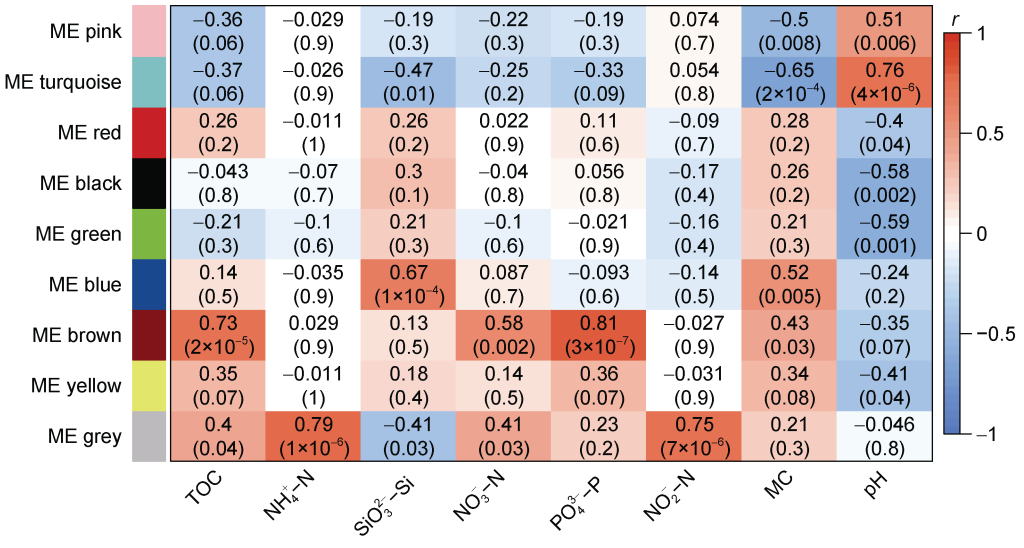

Figure 6 Relationship between bacterial community structure and soil physicochemical factors. The horizontal axis represents the physicochemical factors and the vertical axis represents the bacterial modules. Red shading indicates a positive correlation and blue shading indicates a negative correlation. The darker the color, the stronger the correlation.

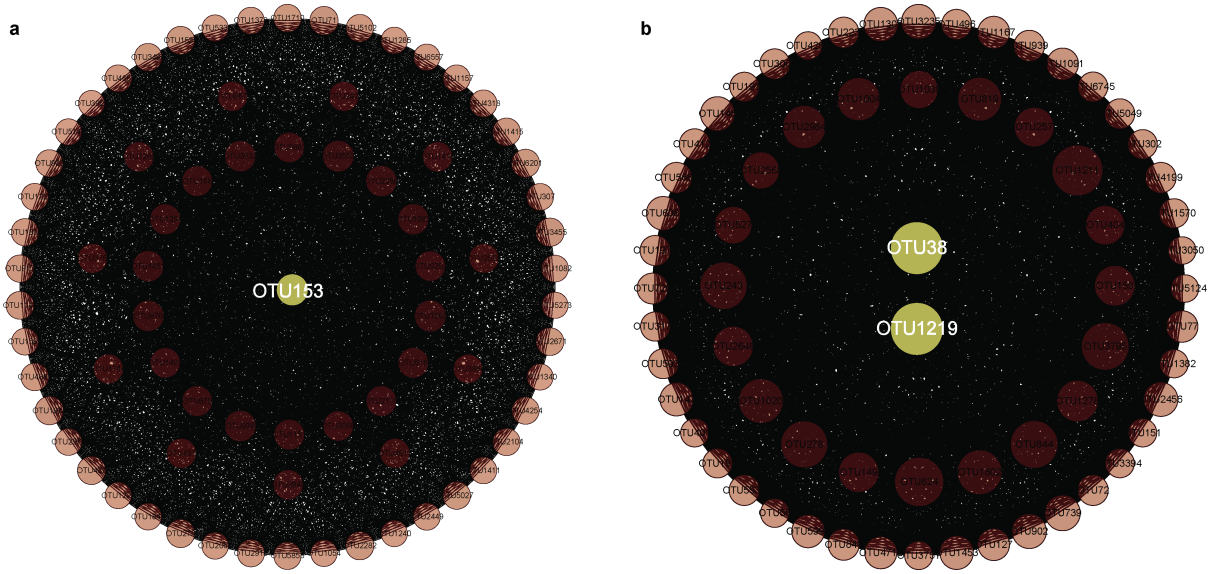

Figure 7 WGCNA network diagrams for the brown and turquoise modules. **a**, brown module; **b**, turquoise module. Nodes represent OTUs and lines indicate the connections between nodes. The larger the size of a node, the greater its correlation with other nodes.

Through sampling different areas and conducting a bioinformatic analysis, the present study revealed the composition and diversity of the bacterial community in the sparse tundra vegetation near the Antarctic coast. In addition, differences in the bacterial community structure at sites differing in slope and degree of vegetation coverage were analyzed. The results showed that, in the non-vegetated area, Proteobacteria and Acidobacteria are dominant in the bacterial community. Proteobacteria is among the largest and most phenotypically diverse phyla of bacteria (Sharma et al., 2022). Acidobacteria are ubiquitous and among the most abundant bacterial phyla in soils (Conradie and Jacobs, 2021). One reason that Proteobacteria can be among the most abundant bacterial phyla in certain oligotrophic environments (Teehera et al., 2018) may lie in their remarkable nitrogen-fixing capabilities (Ding and Sun, 2025). Nitrogen is an essential element for microorganisms (Liu et al., 2020). Acidobacteria were dominant in non-vegetated areas, possibly because a large number of oligotrophic bacteria belonging to the Acidobacteria were detected at the sampling sites. These bacteria inhabit oligotrophic environments and can efficiently utilize elements such as carbon and nitrogen.

Considering the bacterial community composition at the genus rank, ZB1 and ZB2 in the vegetated area were dominated by *Sphingomonas*. As a ubiquitous aerobic bacterium, *Sphingomonas* frequently occurs in aquatic environments (Wallner et al., 2016). As indicated by the soil physicochemical properties at the sampling sites (Figure 2), in the vegetated area, the MC at ZB1 and ZB2 was higher than that at ZB3 and ZB4. This result strongly supports the view that sites ZB1 and ZB2 in the vegetated area are dominated by *Sphingomonas*, and this bacterium—a ubiquitous aerobic bacterium—frequently occurs in aquatic environments. However, the MC of WZB5 and WZB4 in the non-vegetated area was significantly higher than that at the other sampling sites in the non-vegetated area, and differed little from the MC at ZB1 and ZB2 in the vegetated area. The relative abundance of *Sphingomonas* in the vegetated area was substantially lower than that at the sampling sites in the non-vegetated area, probably because the soil in the latter sampling sites was loose, and no lichens and mosses were present in the non-vegetated area to assist in preventing the loss of rainwater. Therefore, the MC on the lower slope was higher than that on the upper slope.

The sites WZB1, WZB2, and WZB3 in the non-vegetated area exhibited minimal variation in soil physicochemical properties (Figure 3). However, their bacterial community structures differed distinctly (Figure 4). In addition, no significant differences in soil physicochemical properties were detected among ZB1, ZB2, ZB3, and ZB4 in the vegetated area, but the bacterial community structure varied substantially. The relative abundance of Gemmatimonadaceae was highest in the soil at the foot of the slope and at the foot of the mountain, and was much lower than that of Sphingomonadaceae in the soil at the top of the mountain and on the slope. We speculate that the difference in the bacterial community structure between the upper- and lower-slope areas might be caused by rainwater erosion.

Biological soil crusts can occur in all biological communities, especially in arid regions and even in extreme environments (Colesie et al., 2014). These crusts are composed of lichens, mosses, algae, and other organisms associated with the surface soil (Antoninka et al., 2020). The crusts play a role in increasing soil organophosphorus content (Concostrina-Zubiri et al., 2022), soil stabilization (Moreira-Grez et al., 2019), and driving the soil carbon cycle (Guan et al., 2022) in dryland ecosystems. The vegetation coverage and development of biological soil

crusts have led to significant differences in the soil physicochemical properties between the vegetated and non-vegetated areas, which in turn has resulted in different bacterial community structures.

In this study, we used WGCNA to evaluate the influence of soil physicochemical factors on the bacterial community structure and determined the core bacterial flora. The results showed that two modules (turquoise and brown) were significantly correlated with multiple soil physicochemical properties. The core flora of the turquoise module were Chthoniobacterales and Chitinophagales, which were significantly positively correlated with the soil pH. The core flora of the brown module was Actinobacteria, which was significantly positively correlated with TOC and PO_4^{3-}-P. Actinobacteria, among the most widely distributed bacterial phyla in soils, is renowned for its remarkable ability to degrade plant residues in vitro (Bao et al., 2021). Genes encoding crucial enzymes responsible for nitrogen fixation from inorganic to organic forms are present in Actinobacteria (Jiao et al., 2021), which may explain the observed correlation between Actinobacteria and TOC. Some Actinobacteria possess the ability to mobilize phosphorus (Vargas Hoyos et al., 2021), which also supports the present finding that *Actinobacteria* was correlated with PO_4^{3-}-P. In addition, certain species of the genus *Sediminibacterium* are capable of oxidizing and reducing iron, a process that affects the environmental pH. This physiological characteristic is consistent with the correlation we observed between *Sediminibacterium* and pH (Zhang et al., 2020).

Recent research on Antarctic microorganisms has mainly focused on themes such as the interactions between phytoplankton and planktonic bacteria in waters near Antarctica (Pavlovska et al., 2025), the microbial communities inhabiting different body parts of Antarctic organisms (Botsidou et al., 2025), and the impact of human trampling on soil microbial communities at sampling sites (Fernández-Martínez et al., 2025). However, there is a lack of research on how slopes affect bacterial community structure. The present study addresses this knowledge gap.

4.2 Limitations of this study and future plans

Although this study contributes novel insights into factors that affect bacterial community structure in Antarctica, it has several limitations. The sampling sites in this study were selected near the southern coastline of Fildes Peninsula, Antarctica. It is presently uncertain whether the collected samples are generalizable to a broader geographic area. In addition, all samples were collected at a single time point, without repeated sampling over an extended period.

To mitigate these limitations, we plan to conduct a functional metagenomic analysis to provide a more detailed picture of the functional capabilities of the microbial communities. We will review relevant literature for studies with sampling sites similar to those in the present research to conduct a longitudinal analysis over time.

5 Conclusion

The present findings suggest that the differences in bacterial community structure on different parts of slopes might be caused by rainwater erosion. Differences in the bacterial community structure between the vegetated and non-vegetated areas might reflect that the formation of biological crusts changes the soil physicochemical properties, thereby impacting the bacterial community composition. WGCNA analysis of the correlation between bacterial modules and soil physicochemical factors, revealed the hub bacteria for modules showing the strongest correlations.

Acknowledgements This project was supported by the National Natural Science Foundation of China (Grant no. 32501365) and Natural Science Foundation of Shandong Province, China (Grant no. ZR2025QC1456). We thank the Guest Editor Dr. Li Liao and anonymous reviewers for their constructive comments.

References

Antoninka A, Faist A, Rodriguez-Caballero E, et al. 2020. Biological soil crusts in ecological restoration: emerging research and perspectives. Restor Ecol, 28(S2): S3-S8, doi: 10.1111/rec.13201.

Asplund J, van Zuijlen K, Roos R E, et al. 2022. Divergent responses of functional diversity to an elevational gradient for vascular plants, bryophytes and lichens. J Veg Sci, 33(1): e13105, doi: 10.1111/jvs.13105.

Bao Y Y, Dolfing J, Guo Z Y, et al. 2021. Important ecophysiological roles of non-dominant Actinobacteria in plant residue decomposition, especially in less fertile soils. Microbiome, 9(1): 84, doi: 10.1186/s40168-021-01032-x.

Botsidou P, Schloter M, Maraci Ö, et al. 2025. Skin, but not gut, microbial communities vary with social density in Antarctic fur seals. Front Microbiol, 16: 1603500, doi: 10.3389/fmicb.2025.1603500.

Colesie C, Gommeaux M, Green T G, et al. 2014. Biological soil crusts in continental Antarctica: Garwood Valley, Southern Victoria Land, and Diamond Hill, Darwin Mountains Region. Antart Sci, 26(2): 115-123, doi: 10.1017/s0954102013000291.

Colesie C, Walshaw C V, Sancho L G, et al. 2023. Antarctica's vegetation in a changing climate. WIREs Clim Change, 14(1): e810, doi: 10.1002/wcc.810.

Concostrina-Zubiri L, Berdugo M, Valencia E, et al. 2022. Decomposition of dryland biocrust-forming lichens and mosses contributes to soil nutrient cycling. Plant Soil, 481(1): 23-34, doi: 10.1007/s11104-022-05481-7.

Conradie T A, Jacobs K. 2021. Distribution patterns of Acidobacteriota in different fynbos soils. PLoS One, 16(3): e0248913, doi: 10.1371/journal.pone.0248913.

de Scally S Z, Makhalanyane T P, Frossard A, et al. 2016. Antarctic microbial communities are functionally redundant, adapted and resistant to short term temperature perturbations. Soil Biol Biochem, 103: 160-170, doi: 10.1016/j.soilbio.2016.08.013.

Ding C L, Sun J. 2025. The potential contribution of microbial communities to carbon fixation and nitrogen cycle in the Eastern Indian Ocean. Mar Environ Res, 207: 107056, doi: 10.1016/j.marenvres.2025.107056.

Dong W X, Cui Z G, Zhao M J, et al. 2023. Seasonal and spatial variations of bacterial community structure in the Bailang River Estuary. J Mar Sci Eng, 11(4): 825, doi: 10.3390/jmse11040825.

Fernández-Martínez M Á, Galbo Cacha R M, López-Archilla A I, et al. 2025. Findings and challenges in understanding the impacts of human-induced trampling on Antarctic edaphic microbial communities and their recovery potential. Antarct Sci: 1-4, doi: 10.1017/s0954102024000531.

Gao X Z, Huang C, Rao K F, et al. 2018. Occurrences, sources, and transport of hydrophobic organic contaminants in the waters of Fildes Peninsula, Antarctica. Environ Pollut, 241: 950-958, doi: 10.1016/j.envpol.2018.06.025.

Guan C, Chen N, Qiao L J, et al. 2022. Contrasting effects of biological soil crusts on soil respiration in a typical steppe. Soil Biol Biochem, 169: 108666, doi: 10.1016/j.soilbio.2022.108666.

Henriques D K, Silva B G C, Zuñiga G E, et al. 2018. Contributions to the bryological knowledge of ASPA 125, Fildes Peninsula, King George Island. Biol Res, 51(1): 29, doi: 10.1186/s40659-018-0178-3.

Ji L, Zhang H Y, Wang Z Y, et al. 2024. Temperature alters bacterial community structure in sediment of mountain stream. Sci Rep, 14(1): 31159, doi: 10.1038/s41598-024-82497-2.

Jiao J Y, Fu L, Hua Z S, et al. 2021. Insight into the function and evolution of the Wood-Ljungdahl pathway in Actinobacteria. ISME J, 15(10): 3005-3018, doi: 10.1038/s41396-021-00935-9.

Kobierski M, Lemanowicz J, Wojewódzki P, et al. 2020. The effect of organic and conventional farming systems with different tillage on soil properties and enzymatic activity. Agronomy, 10(11): 1809, doi: 10.3390/agronomy10111809.

Lebre P H, Bosch J, Coclet C, et al. 2023. Expanding Antarctic biogeography: microbial ecology of Antarctic island soils. Ecography, 2023(9): e06568, doi: 10.1111/ecog.06568.

Li Q X, Wang N F, Han W B, et al. 2022. Soil geochemical properties influencing the diversity of bacteria and Archaea in soils of the Kitezh Lake Area, Antarctica. Biology, 11(12): 1855, doi: 10.3390/biology11121855.

Li S X, Peng Y Y, Li M Y, et al. 2025. Different active exogenous carbons improve the yield and quality of roses by shaping different bacterial communities. Front Microbiol, 16: 1558322, doi: 10.3389/fmicb.2025.1558322.

Liu M, Adl S, Cui X Y, et al. 2020. In situ methods of plant-microbial interactions for nitrogen in rhizosphere. Rhizosphere, 13: 100186, doi: 10.1016/j.rhisph.2020.100186.

Maria Teixeira Lins C, Rodrigues de Souza E, Emanuelle Monteiro dos Santos Souza T, et al. 2023. Influence of vegetation cover and rainfall intensity on soil attributes in an area undergoing desertification in Brazil. Catena, 221: 106751, doi: 10.1016/j.catena.2022.106751.

Moreira-Grez B, Tam K, Cross A T, et al. 2019. The bacterial microbiome associated with arid biocrusts and the biogeochemical influence of biocrusts upon the underlying soil. Front Microbiol, 10: 2143, doi: 10.3389/fmicb.2019.02143.

Niem J M, Billones-Baaijens R, Stodart B, et al. 2020. Diversity profiling of grapevine microbial endosphere and antagonistic potential of endophytic *Pseudomonas* against grapevine trunk diseases. Front Microbiol, 11: 477, doi: 10.3389/fmicb.2020.00477.

Perera-Castro A V, Waterman M J, Turnbull J D, et al. 2020. It is hot in the Sun: Antarctic mosses have high temperature optima for photosynthesis despite cold climate. Front Plant Sci, 11: 1178, doi: 10.3389/fpls.2020.01178.

Pavlovska M, Zotov A, Prekrasna-Kviatkovska Y, et al. 2025. Dynamics of microbial communities in Western Antarctic Peninsula waters shaped primarily by the biological interactions. Front Microbiol, 16: 1591986, doi: 10.3389/fmicb.2025.1591986.

Qin Y L, Wang N F, Zheng L, et al. 2023. Study of archaeal diversity in the Arctic meltwater lake region. Biology, 12(7): 1023, doi: 10.3390/biology12071023.

Qu M X, Duan W B, Chen L X. 2024. The role of cryptogams in soil property regulation and vascular plant regeneration: a review. Appl Sci, 14(1): 2, doi: 10.3390/app14010002.

Roldán D M, Carrizo D, Sánchez-García L, et al. 2022. Diversity and effect of increasing temperature on the activity of methanotrophs in sediments of Fildes Peninsula freshwater lakes, King George Island, Antarctica. Front Microbiol, 13: 822552, doi: 10.3389/fmicb.2022.822552.

Samaddar S, Chatterjee P, Truu J, et al. 2019. Long-term phosphorus limitation changes the bacterial community structure and functioning in paddy soils. Appl Soil Ecol, 134: 111-115, doi: 10.1016/j.apsoil.2018.10.016.

Sharma V, Vashishtha A, Jos A L M, et al. 2022. Phylogenomics of the phylum Proteobacteria: resolving the complex relationships. Curr Microbiol, 79(8): 224, doi: 10.1007/s00284-022-02910-9.

Singh J, Singh R P, Khare R. 2018. Influence of climate change on Antarctic flora. Polar Sci, 18: 94-101, doi: 10.1016/j.polar.2018.05.006.

Teehera K B, Jungbluth S P, Onac B P, et al. 2018. Cryogenic minerals in Hawaiian lava tubes: a geochemical and microbiological exploration. Geomicrobiol J, 35(3): 227-241, doi: 10.1080/01490451.2017.1362079.

Vargas Hoyos H A, Chiaramonte J B, Barbosa-Casteliani A G, et al. 2021. An actinobacterium strain from soil of cerrado promotes phosphorus solubilization and plant growth in soybean plants. Front Bioeng Biotechnol, 9: 579906, doi: 10.3389/fbioe.2021.579906.

Vignon É, Roussel M L, Gorodetskaya I V, et al. 2021. Present and future of rainfall in Antarctica. Geophys Res Lett, 48(8): e2020GL092281, doi: 10.1029/2020GL092281.

Wallner J, Frei R, Burkhalter F. 2016. A rare case of peritoneal dialysis-associated peritonitis with *Sphingomonas koreensis*. Perit Dial Int, 36(2): 224-225, doi: 10.3747/pdi.2015.00065.

Wang M, Wang L, Li Q, et al. 2021. Nitrogen fertilizer driven bacterial community structure in a semi-arid region of Northeast China. Sustainability, 13(21): 11967, doi: 10.3390/su132111967.

Wang N F, Zhang T, Zhang F, et al. 2015. Diversity and structure of soil bacterial communities in the Fildes Region (maritime Antarctica) as revealed by 454 pyrosequencing. Front Microbiol, 6: 1188, doi: 10.3389/fmicb.2015.01188.

Xiang Y W, Dong Y Q, Zhao S Y, et al. 2020. Microbial distribution and diversity of soil around a manganese mine area. Water Air Soil Pollut, 231(10): 506, doi: 10.1007/s11270-020-04878-3.

Zhang T, Ji Z Q, Li J, et al. 2022. Metagenomic insights into the antibiotic resistome in freshwater and seawater from an Antarctic ice-free area. Environ Pollut, 309: 119738, doi: 10.1016/j.envpol.2022.119738.

Zhang W H, Jia X R, Chen S, et al. 2020. Response of soil microbial communities to engineered nanomaterials in presence of maize (*Zea mays* L.) plants. Environ Pollut, 267: 115608, doi: 10.1016/j.envpol.2020.115608.

Zhao M M, Du S S, Li Q H, et al. 2017. High throughput 16S rRNA gene sequencing reveals the correlation between Propionibacterium acnes and sarcoidosis. Respir Res, 18(1): 28, doi: 10.1186/s12931-017-0515-z.